

RESEARCH ACTIVITIES VIII

Coordination Chemistry Laboratories

Prof. Kazushi Mashima (Osaka Univ.) and Assoc. Prof. Masato Kurihara (Yamagata Univ.) took the position of Laboratory of Complex Catalyst from April 2004. Prof. Masahito Yamashita (Tokyo Metropolitan Univ.) and Prof. Naoto Chatani (Osaka Univ.) finished their term as Adjunct Prof. of Complex Catalyst in March 2004. Their effort during their term is gratefully appreciated. Prof. Hiroyuki Matsusaka (Osaka Prefecture Univ.) and Prof. Keiji Ueno (Gunma Univ.) continue the position of the Laboratory of Coordination Bond.

VIII-A Nano-Sciences of Advanced Metal Complexes

Recently, nano-sciences or nano-technologies have been attracting much attention because they show very interesting physical properties based on the non-linearity and quantum effect. There are two methods to obtain the nano-size materials, that is, "top-down" and "bottom-up" methods. The top-down method such as laser abrasion has a limitation to make particles with the sizes less than 100 nm. On the other hand, the bottom-up method is promising to control the nano-size since the chemical reactions are available. However, the researches based on the bottom-up methods are rare and such methods have not been accomplished so far. Then, I would like to focus on the bottom-up methods. As for the bottom-up methods, there are three types of the target materials such as inorganic compounds, organic compounds, and metal complexes. The inorganic compounds easily take three-dimensional bulk structures. The organic compounds easily take 0- and 1-dimensional bulk materials. Therefore, neither inorganic nor organic compounds are suitable for the nano-sciences. On the other hand, the metal complexes easily take nano-size clusters where they are surrounded with the organic ligands. Therefore, the nano-sciences of the advanced metal complexes are most promising. As for the non-linearity, we focus on the gigantic third-order optical non-linearity. As for the quantum effect, we focus on the single-molecule magnets, nano-wire molecule-magnets, and nano-network molecule-magnets.

VIII-A-1 A Three-Dimensional Ferrimagnet Composed of Mixed-Valence Mn_4 Clusters Linked by an $\{Mn[N(CN)_2]_6\}^{4-}$ Unit

MIYASAKA, Hitoshi¹; NAKATA, Kazuya¹; SUGIURA, Ken-ichi¹; YAMASHITA, Masahiro²; CLÉRAC, Rodolphe³

(¹Tokyo Metropolitan Univ.; ²IMS and Tokyo Metropolitan Univ.; ³Cent. Recherche Paul Pascal)

[*Angew. Chem., Int. Ed.* **43**, 707–711 (2004)]

A ferrimagnet with a 3D molecular network has been synthesized and characterized. This compound is composed of units of mixed-valence Mn_4 clusters, a unit that is well known for its single-molecule magnet properties, and Mn^{II} paramagnetic units. Both building blocks are linked by dicyanamide bridging ligand to form a covalent-bonded three-dimensional network. The compound becomes a ferrimagnet at 4.1 K that exhibits a spin-flip phenomenon under the influence of a magnetic field.

VIII-A-2 A Dimeric Manganese(III) Tertdentate Schiff Base Complex as a Single-Molecule Magnet

MIYASAKA, Hitoshi¹; CLÉRAC, Rodolphe²; WERNSDORFER, Wolfgang³; LECREN, Lollita²; BONHOMME, Claire²; SUGIURA, Ken-ichi¹; YAMASHITA, Masahiro⁴

(¹Tokyo Metropolitan Univ.; ²Cent. Recherche Paul Pascal; ³Laboratoire Louis Néel; ⁴IMS and Tokyo

Metropolitan Univ.)

[*Angew. Chem., Int. Ed.* **43**, 2801–2805 (2004)]

The complex $[Mn_2(\text{saltmen})_2(\text{ReO}_4)_2]$ ($\text{saltmen}^{2-} = N,N'-(1,1,2,2\text{-tetramethylethylene})\text{bis}(\text{salicylideneimine})$) is a simple out-of-plane dimer of Mn^{III} ions that unambiguously exhibits single-molecule magnetic behavior. To date, this compound is the smallest magnetic unit which has been reported to behave as a magnet at the molecular level and to show quantum tunneling.

VIII-A-3 Tuning the Electronic Structure from Charge-Transfer Insulator to Mott-Hubbard and Peierls Insulators in One-Dimensional Halogen-Bridged Mixed-Metal Compounds

MATSUZAKI, Hiroyuki¹; IWANO, Kaoru²; AIZAWA, Takumi¹; ONO, Madoka¹; KISHIDA, Hideo¹; YAMASHITA, Masahiro³; OKAMOTO, Hiroshi¹

(¹Univ. Tokyo; ²KEK; ³IMS and Tokyo Metropolitan Univ.)

[*Phys. Rev. B* **70**, 035204 (6 pages) (2004)]

The electronic structures of one-dimensional (1D) halogen-bridged mixed-metal compounds, $[Ni_{1-x}Pd_x(\text{chxn})_2X]X_2$ ($\text{chxn} = \text{cyclohexanediamine}$; $X = \text{Cl, Br}$; $0 < x < 1$), are investigated through optical and magnetic measurements. The results reveal that the system changes from charge-transfer (CT) insulator to Mott-

Hubbard (MH) insulator at around $x \sim 0.3$, and from MH insulator to Peierls insulator at $x \sim 0.9$ with increasing x . From the analysis of optical conductivity spectra using the 1D two-band extended Peierls-Hubbard model, electronic parameters such as Coulomb repulsion energy, pd hybridization, CT energy, and electron-lattice interaction are determined.

VIII-A-4 A Square Cyclic Porphyrin Dodecamer: Synthesis and Single-Molecule Characterization

KATO, Aiko¹; SUGIURA, Ken-ichi¹; MIYASAKA, Hitoshi¹; TANAKA, Hiroyuki²; KAWAI, Tomoji²; SUGIMOTO, Manabu³; YAMASHITA, Masahiro⁴
(¹Tokyo Metropolitan Univ.; ²Osaka Univ.; ³Kumamoto Univ.; ⁴IMS and Tokyo Metropolitan Univ.)

[*Chem. Lett.* **33**, 578–579 (2004)]

We prepared a square cyclic porphyrin dodecamer via the tetramerization of a trimer shaped like a right angle. The molecule was visualized by scanning tunneling microscopy to be square.

VIII-A-5 Visualization of Local Valence Structure in Quasi-One-Dimensional Halogen-Bridged Complexes $[\text{Ni}_{1-x}\text{Pd}_x(\text{chxn})_2\text{Br}]\text{Br}_2$ by STM

TAKAISHI, Shinya¹; MIYASAKA, Hitoshi¹; SUGIURA, Ken-ichi¹; YAMASHITA, Masahiro²; MATSUZAKI, Hiroyuki³; KISHIDA, Hideo³; OKAMOTO, Hiroshi³; TANAKA, Hisaaki⁴; MARUMOTO, Kazuhiro⁴; ITO, Hiroshi⁴; KURODA, Shin-ichi⁴; TAKAMI, Tomohide⁵
(¹Tokyo Metropolitan Univ.; ²IMS and Tokyo Metropolitan Univ.; ³Univ. Tokyo; ⁴Nagoya Univ.; ⁵Visionarts Res. Inc.)

[*Angew. Chem., Int. Ed.* **43**, 3171–3175 (2004)]

we have visualized the Mott-Hubbard and CDW states in quasi-1D halogen-bridged Ni and Pd complexes, respectively. In addition, we succeeded in visualizing the propagation of CDW coherence and the spin soliton in real space in the mixed-metal complexes $[\text{Ni}_{1-x}\text{Pd}_x(\text{chxn})_2\text{Br}]\text{Br}_2$ for the first time.

VIII-A-6 A Dinuclear Ruthenium(II) Chelating Amido Complex: Synthesis, Characterization, and Coupling Reaction with Carbon Monoxide

TAKEMOTO, Shin¹; OSHIO, Shinya¹; KOBAYASHI, Tomoharu¹; MATSUZAKA, Hiroyuki²; HOSHI, Masatsugu³; OKIMURA, Hironobu³; YAMASHITA, Masayo³; MIYASAKA, Hitoshi³; ISHII, Tomohiko³; YAMASHITA, Masahiro⁴
(¹Osaka Prefecture Univ.; ²IMS and Osaka Prefecture Univ.; ³Tokyo Metropolitan Univ.; ⁴IMS and Tokyo Metropolitan Univ.)

[*Organometallics* **23**, 3587–3589 (2004)]

$[\text{CpRuCl}]_4$ ($\text{Cp} = \eta^5\text{-C}_5\text{Me}_5$) reacts with 2 equiv of dilithium 2,3-naphthalenediamide to afford the dinuclear bridging amido complex $[(\text{CpRu})_2\{\mu_2\text{-(NH)}_2\text{-C}_{10}\text{H}_6\}]$ (**1b**) in moderate yield. Treatment of **1b** with CO (1 atm) resulted in the incorporation of three molecules of CO into the diruthenium core to give the carbamoyl amido bis(carbonyl) complex $[\text{CpRu}(\mu_2\text{-CO})\text{-}\{\mu_2\text{-2,3-(CONH)(NH)C}_{10}\text{H}_6\}\text{RuCp(CO)}]$.

VIII-B Early Transition Metal Chemistry Directed to Olefin Polymerization

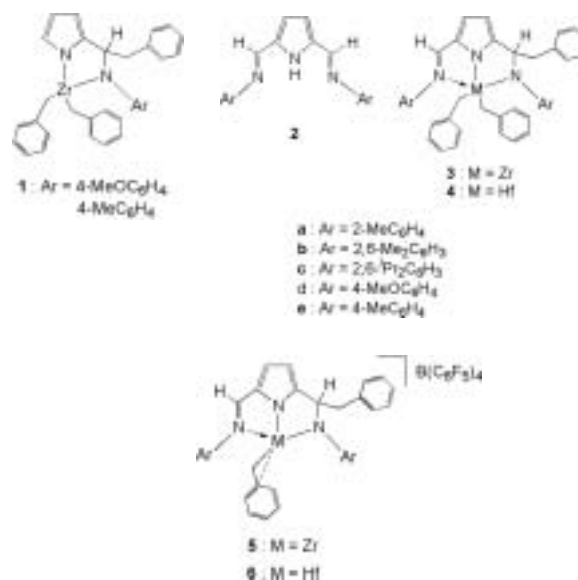
Recent development of well-defined single site transition metal catalysts enables us to precisely control not only catalytic activity for α -olefin polymerization but also microstructure of polymers. The nitrogen-based polydentate ligands such as phenoxyimine, 2,6-bis(*N*-aryliminomethyl)pyridine, and α -diimine derivatives, which serve the polymerization catalysts as supporting ligands, have attracted particular interest in terms of their advantageous feasibility and flexibility in design to introduce sterically and electronically demanding features on the ligand. Despite these merits, the catalysts supported by these ligands have been found to be occasionally deactivated by the alkylation of the C=N bond of the ligand. The alkylation of the C=N moiety of the nitrogen-based ligand was thus anticipated to have a capability to make a cationic alkyl species more stable and, in particular case, enhance its catalytic activity compared to the corresponding catalyst bearing the unalkylated ligand. In this contribution, we have investigated such the alkylation of the ligand related to the polymerization activity and mechanism.

VIII-B-1 Intramolecular Benzoylation of an Imino Group of Tridentate 2,5-Bis(*N*-aryliminomethyl)pyrrolyl Ligands Bound to Zirconium and Hafnium Gives Amido-Pyrrolyl Complexes That Catalyze Ethylene Polymerization

TSURUGI, Hayato¹; YAMAGATA, Tsuneaki¹; MASHIMA, Kazushi²
(¹Osaka Univ.; ²IMS and Osaka Univ.)

[*Organometallics* **23**, 2797–2805 (2004)]

We already reported that an intramolecular benzoylation of the imino moiety of bidentate iminopyrrolyl ligands afforded an amido-pyrrolyl complexes **1** and they exhibited better catalytic activity for ethylene polymerization compared to the corresponding bis-(iminopyrrolyl) dichloro complexes of zirconium. In this contribution, we prepared amido-pyrrolyl complexes of zirconium (**3a-d**) and hafnium (**4a-f**) by the reaction of tetrabenzyl-zirconium and -hafnium with 2,5-bis(*N*-aryliminomethyl)pyrrole ligands (**2a-e**), respectively. During the course of the reaction, one of two imino moieties of the ligand was selectively benzoylated to give unique dianionic tridentate ligands, which stabilized dibenzyl complexes of zirconium and hafnium. The coordinative unsaturation around the metal center was compensated by not only the donation of the imino moiety but also the η^2 -coordination of one of the two benzyl ligands, as confirmed by spectral data together with X-ray analysis of **3b** and **3c**. The zirconium complexes **3b** and **3c** bearing bulky substituents at the nitrogen atoms of the ligand exhibited high catalytic activities (**3b**, 131 (kg-PE)(mol-cat)⁻¹h⁻¹ at 60 °C; **3c**, 458 (kg-PE)(mol-cat)⁻¹h⁻¹ at 75 °C) upon combined with 1000 equiv. of MMAO. Lewis-base free cationic alkyl complexes **5b**, **5c**, **6b**, and **6c** were prepared by alkyl abstraction from the corresponding dibenzyl complexes of zirconium **3b,c** and hafnium **4b,c** and the resulting cationic complexes **5c** and **6c** were found to catalyze the ethylene polymerization without MMAO.



VIII-C Linear Metal Clusters: Bonding and Reactivity

Assembled metal complexes with highly controlling their nuclearity and dimensionality have extensively investigated and quasi-one-dimensional materials, especially transition-metal linear-chain complexes, have attracted particular interest in view of their novel electronic, magnetic, and optical properties. In this contribution, we prepared two linear chain compounds comprised of Mo–Mo multiple bond in their chain.

VIII-C-1 An Infinite Zigzag Chain of Alternating Cl–Pd–Pd–Cl and Mo–Mo Units

MASHIMA, Kazushi¹; YI, JianJun²;
MIYABAYASHI, Takayuki²; OHASHI, Masato²;
YAMAGATA, Tsuneaki²
(¹IMS and Osaka Univ.; ²Osaka Univ.)

[*Inorg. Chem.* **43**, 6596–6599 (2004)]

Treatment of Pd₂Cl₂(CNC₆H₃Me₂-2,6)₄ (**1**) and Mo₂(O₂CCF₃)₄ (**2**) in dichloromethane afforded an infinite zigzag chain $\{[\text{Pd}_2\text{Cl}_2(\text{CNC}_6\text{H}_3\text{Me}_2-2,6)_4][\text{Mo}_2(\text{O}_2\text{CCF}_3)_4]\}_n$ (**3**), where two metal–metal bonded dinuclear Pd–Pd and Mo–Mo units were bridged by chloro atoms (equation 1). The Mo–Mo distance (2.1312(3) Å) of **3** is significantly elongated compared to that of **2** (2.090(4)) Å and lies in the range of that of the quadruple Mo–Mo bonded complexes (Figure 1). Such the elongation might be attributed to the axial donation of the chloro atoms of the Pd–Pd unit to the Mo–Mo moiety.

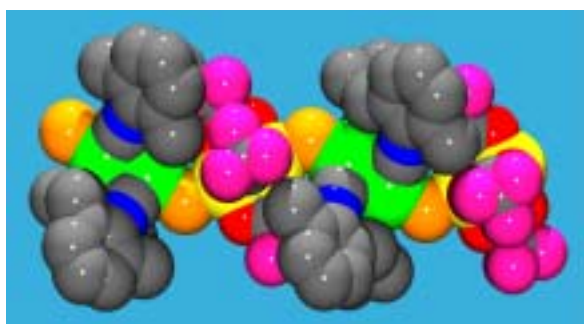
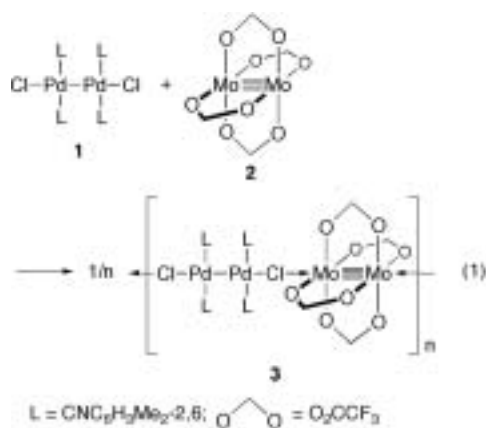


Figure 1. The structure of the infinite zigzag chain of **3**. Mo: yellow; Pd: green; Cl: orange; F: purple; O: red; N: blue; C: gray.

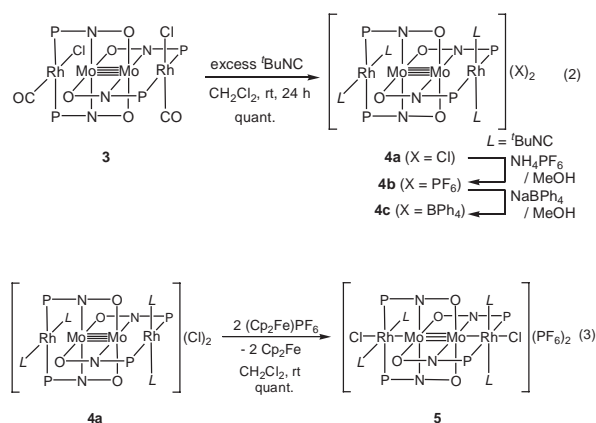
VIII-C-2 Unique Oxidative Metal–Metal Bond Formation of Linearly Aligned Tetranuclear Rh–Mo–Mo–Rh Clusters

MASHIMA, Kazushi¹; RÜFFER, Tobias²; OHASHI, Masato²; SHIMA, Asuka²; MIZUMOTO, Hitoshi²;
KANEDA, Yutaka²
(¹IMS and Osaka Univ.; ²Osaka Univ.)

[*J. Am. Chem. Soc.* **126**, 12244–12245 (2004)]

The construction of one-dimensional, covalently bonded metal strings has attracted much interest in view of fundamental bonding nature as well as promising applications as extensive electronic and optoelectronic materials. Two major synthetic approaches to these compounds have been conducted by (a) using polydentate ligands such as oligo- α -pyridylamido ligands or by (b) partial oxidation of d⁸ square-planar complexes to form metal–metal bonds (*e.g.* platinum blue). Our effort has been focused on aligning transition metals by using a tridentate ligand 6-diphenylphosphino-2-pyridonate (pyphos), in which three different elements, P, N, and O, were linearly laid out by the rigid pyridone framework and could act as coordination sites for arrangement of more than two kinds of transition metals in linear manner. And we have demonstrated linear heterometallic clusters containing both group VI and group X metals by use of the quadruply-bonded dimolybdenum(II) complex, Mo₂(pyphos)₄ (**1**) as a core part of metal strings such as Mo₂Pd₂Cl₂(pyphos)₄ (**2**).

As the next stage of our continuous study, we confronted the synthesis of a new series of heterometallic tetranuclear clusters containing group IX metals with appropriate geometries of square planar as well as octahedral to be supported by the two PPh₂ groups. Herein we report the synthesis of linearly aligned tetranuclear complexes bearing the Rh–Mo–Mo–Rh array (equation 2) and their unique oxidative reaction (equation 3). We found that rhodium metals at both axial positions of the Mo₂ in **4** electronically communicated through the Mo₂ core and, as a result, oxidative reaction Rh(I)/Rh(II) induced the formation of metal–metal bonds.



VIII-D Development of New Transformations Based on a Chelation-Assistance

We have developed a series of catalytic reactions, which involve the facile cleavage of unreactive bonds, such as C–H, C–C, C–F, and C–O bonds by taking advantage of the coordination of the directing group on the transition metals. Heteroatoms, such as carbonyl oxygen or sp^2 nitrogen, function as the directing group, and the coordination of the directing group to transition metals is a key step in those catalytic reactions. Various combination of directing group and catalysts would be expected to be available.

VIII-D-1 Ruthenium-Catalyzed C-H/CO/Olefin Coupling Reaction of *N*-Arylpyrazoles. Extraordinary Reactivity of *N*-Arylpyrazoles toward Carbonylation at C–H Bonds

ASAUMI, Taku²; CHATANI, Naoto¹; MATSUO, Takuya²; KAKIUCHI, Fumitoshi²; MURAI, Shinji²
(¹IMS and Osaka Univ.; ²Osaka Univ.)

[*J. Org. Chem.* **68**, 7538–7540 (2003)]

The reaction of 1-arylpyrazoles with CO and ethylene in the presence of $Ru_3(CO)_{12}$ resulted in regioselective carbonylation at the ortho C–H bonds. While it is found that the pyrazole ring also functions as the directing group for C–H bond cleavage, the efficiency of the reaction depends on position of the pyrazole ring.

VIII-D-2 A Chelation-Assisted Hydroesterification of Alkenes Catalyzed by Rhodium Complex

YOKOTA, Kazuhiko²; TATAMIDANI, Hiroto²; KAKIUCHI, Fumitoshi²; CHATANI, Naoto¹
(¹IMS and Osaka Univ.; ²Osaka Univ.)

[*Org. Lett.* **5**, 4329–4331 (2003)]

The hydroesterification of alkenes with 2-pyridylmethanol catalyzed by $Rh_4(CO)_{12}$ is described. The reaction is accelerated by the presence of a pyridine ring in the alcohol. The reaction is applicable to various alkenes, both terminal and internal alkenes.

VIII-D-3 Ruthenium- and Rhodium-Catalyzed Direct Carbonylation of the *Ortho* C–H Bonds in the Benzene Ring of *N*-Arylpyrazoles

ASAUMI, Taku²; MATSUO, Takuya²; FUKUYAMA, Takahide²; IE, Yutaka²; KAKIUCHI, Fumitoshi²; CHATANI, Naoto¹
(¹IMS and Osaka Univ.; ²Osaka Univ.)

[*J. Org. Chem.* **69**, 4433–4440 (2004)]

The direct carbonylation of C–H bonds in the benzene ring of *N*-phenylpyrazoles *via* catalysis by ruthenium or rhodium complexes is described. The reaction of *N*-phenylpyrazoles with carbon monoxide and ethylene in the presence of $Ru_3(CO)_{12}$ or $Rh_4(CO)_{12}$ resulted in the siteselective carbonylation of the *ortho* C–H bonds in the benzene ring to give the corresponding

ethyl ketones. A variety of functional groups on the benzene ring can be tolerated. *N*-Phenylpyrazoles have higher reactivities than would be expected, based on the pK_a values of the conjugate acid of pyrazole. The choice of solvent for this reaction is significant, and *N,N*-dimethylacetamide (DMA) gives the best result.

VIII-D-4 Catalytic Cross-Coupling Reaction of Esters with Organoboron Compounds and Decarbonylative Reduction of Esters with $HCOONH_4$: A New Route to Acyl Transition Metal Complexes through the Cleavage of Acyl-Oxygen Bonds in Esters

TATAMIDANI, Hiroto²; YOKOTA, Kazuhiko²; KAKIUCHI, Fumitoshi²; CHATANI, Naoto¹
(¹IMS and Osaka Univ.; ²Osaka Univ.)

[*J. Org. Chem.* **69**, 5615–5621 (2004)]

The $Ru_3(CO)_{12}$ -catalyzed cross-coupling reaction of esters with organoboron compounds leading to ketones is described. A wide variety of functional groups can be tolerated under the reaction conditions. Aromatic boronates function as a coupling partner to give aryl ketones. Acyl-alkyl coupling to dialkyl ketones is also achieved by the use of 9-alkyl-9-BBN in place of boronates. The $Ru_3(CO)_{12}$ -catalyzed decarbonylative reduction of esters with ammonium formate ($HCOONH_4$) leading to hydrocarbons is also described. No expected aldehydes are produced, and controlled experiments indicate that aldehydes are not intermediate for the transformation. A hydrosilane can also be used as a reducing reagent in place of $HCOONH_4$. A wide variety of functional groups are compatible for both reactions. The key step for both catalytic reactions is the directing group-promoted cleavage of an acyl carbon-oxygen bond in esters, leading to the generation of acyl transition metal alkoxo complexes.

VIII-E Development of Metal-Conjugated Multi-Electron Redox Systems in Metal-Dioxolene Complexes

Dioxolenes act as a versatile electron-acceptor or -donor through the reversible two-electron redox reactions among the three oxidation states of catechol (Cat), semiquinone (SQ), and quinone (Q). The dioxolene ligands offer a wide range of the metal complexes with a unique metal-conjugated intramolecular electron transfer, which is a fascinating nature to design electrocatalysts and electronic molecular devices. The ruthenium-terpyridine-dioxolene complexes exhibit the reversible two-electron redox behavior and each oxidation state has been recognized as a resonance hybrid on account of the accessible redox potentials between the metal center and the dioxolene ligand. Ferrocene-attached dioxolenes through π -conjugation provide a three-electron redox system, in which a new redox state of the ferrocenyl moiety is combined with the general two-electron redox reaction of the dioxolene moiety. The new oxidation state would be noninnocent, because the redox potentials of both moieties are close. Here we report the syntheses of a new ferrocene-attached dioxolene ligand and its ruthenium-terpyridine complex, and the metal-conjugated three reversible redox behavior.

VIII-E- 1 Syntheses of Ferrocenylcatechol and Its Ruthenium-Terpyridine Complex and the Metal-Conjugated Redox Behavior

KURIHARA, Masato¹; OHIZUMI, Tomohiro²;
SAKAMOTO, Masatomi²; WADA, Tohru;
TANAKA, Koji
(¹IMS and Yamagata Univ.; ²Yamagata Univ.)

A ferrocene-attached dioxolene, 4-ferrocenylcatechol (Fc-CatH₂), and its ruthenium-acetato-terpyridine complex, [Ru^{II}(OAc)(SQ-Fc)(ph-terpy)] (**1**), were synthesized (Figure 1), where ph-terpy and SQ-Fc are 4'-phenyl-2,2':6',2''-terpyridine and 4-ferrocenyl-1,2-benzosemiquinone, respectively. The cyclic voltammogram of **1** shows three reversible redox waves at $E_{1/2} = -0.95, -0.15,$ and 0.40 V vs. Ag/Ag⁺, and the three redox couples correspond to (**1**⁻/**1**), (**1**/**1**⁺), and (**1**⁺/**1**²⁺), respectively, based on the rest potential (-0.22 V) of **1**. The UV-Vis-NIR absorption spectra of **1**⁻, **1**, **1**⁺, and **1**²⁺ were investigated by controlled potential electrolyses at $-1.30, -0.33, 0,$ and 0.50 V, respectively. The specific absorption of **1** in near-IR region was derived from superposition of two bands at 862 and 1015 nm. The higher energy band is similar to that of [Ru^{II}(OAc)(SQ)(terpy)] (**2**) (SQ = 1,2-benzosemiquinone and terpy = 2,2':6',2''-terpyridine) at 878 nm, which is assigned to a metal-to-ligand charge transfer (MLCT) band (Ru(II) to SQ). This fact suggests that **1** has a similar structure, [Ru^{II}(OAc)(SQ-Fc)(ph-terpy)], to **2**. The additional near-IR band is ascribable to another MLCT band (Fe(II) of the ferrocenyl group to SQ). In the absorption spectrum of **1**⁺, an intense band at 674 nm appeared and the maximal wavelength is shifted to a lower energy region than that of the MLCT band (Ru(III) to SQ) in [Ru^{III}(OAc)(SQ)(terpy)]⁺ (**2**⁺) at 556 nm. On the other hand, the absorption maximum at 1280 nm of a MLCT band in **1**⁺ is also shifted to a lower energy region compared with that (Fe(II) to SQ) of **1**. The significant lower energy shift of the MLCT bands is understandable by consideration of the metal-conjugated resonance between Ru(III)-SQ-Fc \rightleftharpoons Ru(II)-Q-Fc \rightleftharpoons Ru(II)-SQ-Fc⁺ (Q = 1,2-benzoquinone and Fc⁺ = Fe(III) form). The contribution of Ru(II)-SQ-Fc⁺ and Ru(II)-Q-Fc structures in **1**⁺ is responsible for the lower energy shift of the former and the latter MLCT bands, respectively.

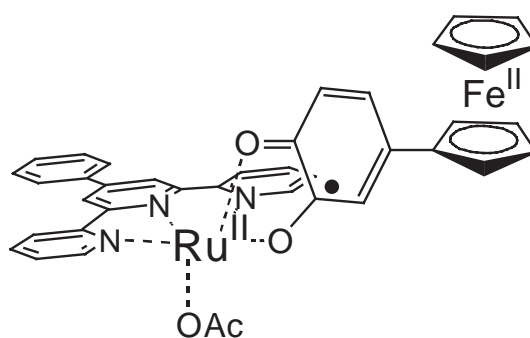


Figure 1. The structure of **1**.

VIII-F Reduction of CO₂ and Oxidation of Organic Molecules Aiming at Energy Conversion between Chemical Energy and Electricity

Electro- and photochemical reduction of CO₂ affording methanol has become crucial issue in line with the progress of fuel energy cells using methanol. Carbon dioxide easily forms η^1 - and η^2 -CO₂ adducts by the reaction with coordinatively unsaturated low-valent metal complexes. Metal complexes with η^1 -CO₂ in protic media are smoothly converted to the corresponding metal-CO ones, which undergo reductive cleavages of the M-CO bonds by accumulation of electrons at the metal centers under electrolysis conditions. A number of metal complexes have proven to catalyze reduction of CO₂ to CO, but the process prevents the CO ligand from hydrogenation leading to methanol formation. To achieve electrochemical reduction of the carbonyl ligand derived from CO₂, we are designing new types of metal complexes that can provide electrons to carbonyl carbon through redox active ligands without increasing electron densities in the metal centers.

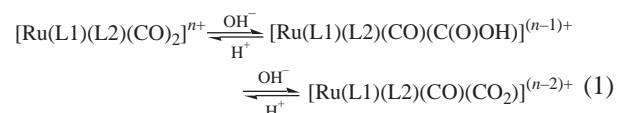
Metal complexes that have an ability to oxidize organic molecules at potentials more negative than the reduction potential of dioxygen enable the direct conversion from chemical energy of organic molecules to electricity. Metal-oxo complexes are possible candidates for the smooth oxidation of organic molecules, since metal-oxo species are believed to work as active centers in various metal enzymes, which oxidize various biological substrates under very mild conditions. Mechanistic understandings of the reactivity of metal-oxo species are limited because of the difficulty of selective formation of reactive M-O frameworks in artificial systems. On the other hand, high valent Ru=O complexes can be obtained by sequential electron and proton loss of the corresponding Ru-OH₂ ones, and have proven to work as oxidants of organic molecules. We have succeeded smooth and reversible conversion between aqua and oxo ligands on Ru-dioxolene frameworks without using any oxidants by taking advantage of dioxolene as a redox active ligand. Along this line, we have been preparing a variety of metal-aqua complexes bearing a dioxolene ligand aiming at oxidation of hydrocarbons by the corresponding metal-oxo forms.

VIII-F-1 Regulation of Electron Donating Ability to Metal Center: Isolation and Characterization of Ruthenium Carbonyl Complexes with N,N- and/or N,O-Donor Polypyridyl Ligands

OOYAMA, Dai¹; KOBAYASHI, Takanori; SHIREN, Kazushi; TANAKA, Koji
(¹Yamagata Univ.)

[*J. Organomet. Chem.* **665**, 107–113 (2003)]

Polypyridyl ruthenium(II) dicarbonyl complexes with an N,O- and/or N,N-donor ligand, [Ru(pic)(CO)₂Cl₂]⁻ (**1**), [Ru(bpy)(pic)(CO)₂]⁺ (**2**), [Ru(pic)₂(CO)₂] (**3**), and [Ru(bpy)₂(CO)₂]²⁺ (**4**) (pic = 2-pyridyl-carboxylato, bpy = 2,2'-bipyridine) were prepared for comparison of the electron donor ability of these ligands to the ruthenium center. Salts of complexes **1** and **2** were characterized by x-ray crystallography. A carbonyl group of [Ru(L1)(L2)(CO)₂]ⁿ⁺ (L1, L2 = bpy, pic) successively reacted with one and two equiv of OH⁻ to form [Ru(L1)(L2)(CO)(C(O)OH)]⁽ⁿ⁻¹⁾⁺ and [Ru(L1)(L2)(CO)(CO₂)]⁽ⁿ⁻²⁾⁺ (eq 1).



These three complexes exist as equilibrium mixtures in aqueous solutions and the equilibrium constants were determined potentiometrically. Electrochemical reduction of **2** in CO₂-saturated CH₃CN-H₂O at -1.5 V selectively produced CO.

VIII-F-2 Mono-Dithiolene Molybdenum(IV) Complexes of *cis*-1,2-Dicyano-1,2-Ethylene-Dithiolate (mnt²⁻): New Models for Molybdenum Enzymes

SUGIMOTO, Hideki; SHIREN, Kazushi; TSUKUBE, Hiroshi; TANAKA, Koji

[*Eur. J. Inor. Chem.* **14**, 2633–2638 (2003)]

New mono-dithiolene Mo(IV) complexes of *cis*-1,2-dicyano-1,2-ethylenedithiolato [(mnt)²⁻] were synthesized as models for Mo enzymes, with 4,4'-di-*tert*-butyl-2,2'-bipyridine (Bu₂bpy) and *N,N'*-tetraethyl-ethylenediamine (Et₄en) as ancillary ligands, and characterized by IR, UV/visible, elemental anal., ESI-mass and electrochemical techniques. The temperature dependent ¹H NMR spectra, recorded in CD₃CN solution, indicated that [MoO(mnt)(Bu₂bpy)] (**1**) has a rigid structure but [MoO(mnt)(Et₄en)] (**2**) showed dynamic conformational inversion processes involving the chelating ethylenediamine unit. The complexes exhibited different reactivity toward O₂: **1** gave a single oxo-bridged dimolybdenum dimer complex [Mo₂O₃(mnt)₂(Bu₂bpy)₂] (**3**), while **2** did not react with O₂ and kept its mononuclear structure. Both complexes have almost the same redox potential for Mo^{IV/V}, and so the steric bulkiness and conformational dynamics probably cause this marked contrast. The obtained dimolybdenum complex **3** was also structurally characterized and studied, and is a new dimolybdenum complex with one dithiolene per Mo. The crystal structure of the starting complex MoO₂Cl₂(Bu₂bpy) (**4**) is also reported.

VIII-F-3 Characterization of a Stable Ruthenium Complex with an Oxyl Radical

KOBAYASHI, Katsuaki; OHTSU, Hideki¹; WADA, Tohru; KATO, Tatsuhisa; TANAKA, Koji
(¹CREST/JST)

[*J. Am. Chem. Soc.* **125**, 6729–39 (2003)]

The ruthenium oxyl radical complex, [Ru^{II}(trpy)(Bu₂SQ)O^{•-}] (trpy = 2,2':6',2''-terpyridine, Bu₂SQ = 3,5-di-*tert*-butyl-1,2-benzosemiquinone) was prepared for the first time by the double deprotonation of the aqua ligand of [Ru^{III}(trpy)(Bu₂SQ)(OH₂)](ClO₄)₂. [Ru^{III}(trpy)(Bu₂SQ)(OH₂)](ClO₄)₂ is reversibly converted to [Ru^{III}(trpy)(Bu₂SQ)(OH⁻)]⁺ upon dissociation of the aqua proton (p*K*_a 5.5). Deprotonation of the hydroxo proton gave rise to intramolecular electron transfer from the resultant O²⁻ to Ru-dioxolene. The resultant [Ru^{II}(trpy)(Bu₂SQ)O^{•-}] showed antiferromagnetic behavior with a Ru^{II}-semiquinone moiety and oxyl radical, the latter of which was characterized by a spin trapping technique. The most characteristic structural feature of [Ru^{II}(trpy)(Bu₂SQ)O^{•-}] is a long Ru–O bond length (2.042(6) Å) as the first terminal metal–O bond with a single bond length. To elucidate the substituent effect of a quinone ligand, [Ru^{III}(trpy)(4ClSQ)(OH₂)](ClO₄)₂ (4ClSQ = 4-chloro-1,2-benzosemiquinone) was prepared and we compared the deprotonation behavior of the aqua ligand with that of [Ru^{III}(trpy)(Bu₂SQ)(OH₂)](ClO₄)₂. Deprotonation of the aqua ligand of [Ru^{III}(trpy)(4ClSQ)(OH₂)](ClO₄)₂ induced intramolecular electron transfer from OH⁻ to the [Ru^{III}(4ClSQ)] moiety affording [Ru^{II}(trpy)(4ClSQ)(OH^{•-})]⁺, which then probably changed to [Ru^{II}(trpy)(4ClSQ)O^{•-}]. The antiferromagnetic interactions (*J* values) between Ru^{II}-semiquinone and the oxyl radical for [Ru^{II}(trpy)(Bu₂SQ)O^{•-}] and for [Ru^{II}(trpy)(4ClSQ)O^{•-}] were *2J* = -0.67 cm⁻¹ and -1.97 cm⁻¹, respectively.

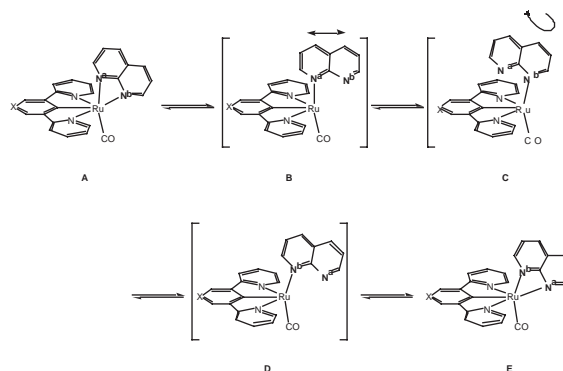
VIII-F-4 Synthesis, Structures and Fluxional Behavior of Ruthenium(II) Complexes Bearing a Bidentate 1,8-Naphthyridine Ligand

KOIZUMI, Take-aki; TOMON, Takashi; TANAKA, Koji

[*Bull. Chem. Soc. Jpn.* **76**, 1969–1975 (2003)]

The Ru complexes bearing 1,8-naphthyridine (napy) and terpyridine analogous (N,C,N)-tridentate ligands were synthesized and characterized. The reaction of [RuCl₂(napy-*k*²*N,N'*)(DMSO)₂] with 2 equiv of AgPF₆ and subsequent addition of LH and CO gave [RuL(napy-*k*²*N,N'*)(CO)](PF₆)_{*n*} (**6a**: L = *N*-methyl-3,5-di(2-pyridyl)-4-pyridyl, *n* = 2; **6b**: L = 2,6-di(2-pyridyl)phenyl, *n* = 1) via [RuL(napy-*k*²*N,N'*)(DMSO)](PF₆)_{*n*} (**5a**: L = *N*-methyl-3,5-di(2-pyridyl)-4-pyridyl, *n* = 2; **5b**: L = 2,6-di(2-pyridyl)phenyl, *n* = 1). The crystal structures of **5a** and **6a** show distorted octahedral coordination with the tridentate (N,C,N)-ligand as mer-fashion, two nitrogens of bidentate napy and the S of DMSO (**5a**) or the C of the CO ligand (**6a**). Detailed expts. for irradiation and variable-temperature ¹H NMR

studies reveal a fluxional process of the chelated napy ligand in solutions.



VIII-F-5 Selective Formation of Inter- and Intramolecular A-D-A π-π Stacking: Solid-State Structures of Bis(pyridiniopropyl)benzenes

KOIZUMI, Take-aki; TSUTSUI, Kanako; TANAKA, Koji

[*Eur. J. Org. Chem.* **23**, 4528–4532 (2003)]

The synthesis and mol. structures of bis(pyridinio-propyl)benzene derivatives [*p*-(4-RC₅H₄N⁺CH₂CH₂CH₂)₂C₆H₄](X⁻)₂ [R = H, X = I (**I**); R = CMe₃, X = Br (**II**)] have been investigated. **I** adopts a linear structure in the solid state and the crystal packing geometry can be defined as isolated triplets formed by the phenylene ring of one mol. and two pyridinium rings of two neighboring molecules. In contrast, **II** has an S-shaped arrangement, and an intramolecular acceptor-donor-acceptor triplet is formed among the central phenylene ring and two terminal pyridinium rings in the same mol. Such a distinct difference in the crystal structures of **I** and **II** can be ascribed to the substituent on the pyridinium unit. The steric repulsion of the bulky *tert*-Bu group hinders internal. A-D-A π-π stacking.

VIII-F-6 Equilibrium of Low- and High-Spin States of Ni(II) Complexes Controlled by the Donor Ability of the Bidentate Ligands

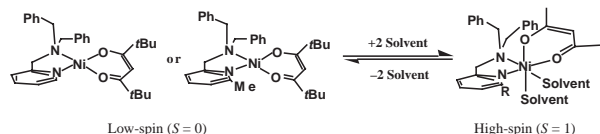
OHTSU, Hideki¹; TANAKA, Koji
(¹IMS, CREST/JST)

[*Inorg. Chem.* **43**, 3024–30 (2004)]

Low-spin nickel(II) complexes containing bidentate ligands with modulated nitrogen donor ability, Py(Bz)₂ or MePy(Bz)₂ (Py(Bz)₂ = *N,N*-bis(benzyl)-*N*-(2-pyridyl)methylamine, MePy(Bz)₂ = *N,N*-bis(benzyl)-*N*-[(6-methyl-2-pyridyl)methyl]amine), and a β-diketone derivative, *t*BuacacH (*t*BuacacH = 2,2,6,6-tetramethyl-3,5-heptanedione), represented as [Ni(Py(Bz)₂)(*t*Buacac)](PF₆) (**1**) and [Ni(MePy(Bz)₂)(*t*Buacac)](PF₆) (**2**) have been synthesized. In addition, the corresponding high-spin nickel(II) complexes having a nitrate ion, [Ni(Py(Bz)₂)(*t*Buacac)(NO₃)] (**3**) and [Ni(MePy(Bz)₂)(*t*Buacac)(NO₃)] (**4**), have also been synthesized for comparison. Complexes **1** and **2** have tetracoordinate

low-spin square-planar structures, whereas the coordination environment of the nickel ion in **4** is a hexacoordinate high-spin octahedral geometry. The absorption spectra of low-spin complexes **1** and **2** in a noncoordinating solvent, dichloromethane (CH_2Cl_2), display the characteristic absorption bands at 500 and 540 nm, respectively. On the other hand, the spectra of a CH_2Cl_2 solution of high-spin complexes **3** and **4** exhibit the absorption bands centered at 610 and 620 nm, respectively. The absorption spectra of **1** and **2** in *N,N*-dimethylformamide (DMF), being a coordinating solvent, are quite different from those in CH_2Cl_2 , which are nearly the same as those of **3** and **4** in CH_2Cl_2 . This result indicates that the structures of **1** and **2** are converted from a low-spin square-planar to a high-spin octahedral configuration by the coordination of two DMF molecules to the nickel ion. Moreover, complex **1** shows thermochromic behavior resulting from the equilibrium between low-spin square-planar and high-spin octahedral structures in acetone, while complex **2** exists only as a high-spin octahedral configuration in acetone at any temperature.

Such drastic differences in the binding constants and thermochromic properties can be ascribed to the enhancement of the acidity of the nickel ion of **2** by the steric effect of the *o*-methyl group in the $\text{MePy}(\text{Bz})_2$ ligand in **2**, which weakens the Ni-N(pyridine) bond length compared with that of the nonsubstituted $\text{Py}(\text{Bz})_2$ ligand in **1**.



VIII-F-7 Acid-Base Equilibria of Various Oxidation States of Aqua-Ruthenium Complexes with 1,10-Phenanthroline-5,6-Dione in Aqueous Media

FUJIHARA, Tetsuaki; WADA, Tohru; TANAKA, Koji

[*Dalton Trans.* 645–52 (2004)]

Syntheses and pH dependent electrochemical properties of aqua-ruthenium(II) complexes, $[\text{Ru}(\text{trpy})(\text{PDA}-N,N')(\text{OH}_2)](\text{ClO}_4)_2$ (**1**)(ClO_4)₂ and $[\text{Ru}(\text{trpy})(\text{PD}-N,N')(\text{OH}_2)](\text{ClO}_4)_2$ (**2**)(ClO_4)₂ (trpy = 2,2':6',2''-terpyridine, PDA = 6-acetonyl-6-hydroxy-1,10-phenanthroline-5-one, PD = 1,10-phenanthroline-5,6-dione) are presented. Treatment of $[\text{Ru}(\text{trpy})(\text{PD}-N,N')\text{Cl}](\text{PF}_6)$ with AgClO_4 in a mixed solvent of acetone and H_2O selectively produced the acetonyl-PD complex **1** (ClO_4)₂, and the similar treatment in a mixed solvent of 2-methoxyethanol and H_2O gave the PD complex **2** (ClO_4)₂. The molecular structures of both complexes were determined by X-ray structural analysis. The proton dissociation constants of various oxidations state of $[\mathbf{1}]^{2+}$ and $[\mathbf{2}]^{2+}$ were evaluated by simulation of $E_{1/2}$ values of those redox potentials depending on pH. The simulation revealed that the acetonyl-PD complex $[\mathbf{1}]^{2+}$ underwent successive Ru(II)/Ru(III) and Ru(III)/Ru(IV)

redox couples though the two redox reactions were not separated in the cyclic voltammograms. The redox behavior of $[\mathbf{2}]^{2+}$ in H_2O is reasonably explained by not only the similar successive metal-centered redox reactions but also simultaneous two-electron quinone/catechol redox couple of the PD ligand including the contribution of hydration on a carbonyl carbon.

VIII-F-8 Syntheses and Electrochemical Properties of Ruthenium(II) Complexes with 4,4'-Bipyrimidine and 4,4'-Bipyrimidinium Ligands

FUJIHARA, Tetsuaki¹; WADA, Tohru; TANAKA, Koji

(¹IMS, CREST/JST)

[*Inorg. Chim. Acta* **357**, 1205–1212 (2004)]

The syntheses and electrochem. properties of novel ruthenium(II) polypyridyl complexes with 4,4'-bipyrimidine, $[\text{Ru}(\text{trpy})(\text{bpm})\text{Cl}](\text{X})$ (**1**)(X; X = PF_6^- , BF_4^-) and with a quaternized 4,4'-bipyrimidinium ligand, $[\text{Ru}(\text{trpy})(\text{Me}_2\text{bpm})\text{Cl}](\text{BF}_4)_3$ (**2**)(BF_4)₃, trpy = 2,2':6',2''-terpyridine, bpm = 4,4'-bipyrimidine, Me₂bpm = 1,1'-dimethyl-4,4'-bipyrimidinium) are presented. The bpm complex **1**⁺ was prepared by the reaction of $\text{Ru}(\text{trpy})\text{Cl}_3$ with 4,4'-bipyrimidine in EtOH/ H_2O . The structural characterization of **1**⁺ revealed that the bpm ligand coordinated to the ruthenium atom in a bidentate fashion. Diquaternization of the noncoordinating nitrogen atoms on bpm of **1**⁺ by Me_3OBF_4 in CH_3CN gave **2**(BF_4)₃. The electrochemical and spectroelectrochemical properties of the complexes are described.

VIII-F-9 Strong Interaction between Carbonyl and Dioxolene Ligands Caused by Charge Distribution of Ruthenium-Dioxolene Frameworks of Mono- and Dicarbonylruthenium Complexes

WADA, Tohru; FUJIHARA, Tetsuaki¹; TOMORI, Mizuno²; OYAMA, Dai²; TANAKA, Koji

(¹IMS, CREST/JST; ²Fukushima Univ.)

[*Bull. Chem. Soc. Jpn.* **77**, 741–749 (2004)]

Monocarbonylruthenium complexes with a semiquinone ligand, $[\text{Ru}(\text{CO})(\text{sq})(\text{L})]^{n+}$ (sq = 3,5-di-*tert*-butyl-1,2-benzosemiquinone, *n* = 1 or 0, L = 2,2':6',2''-terpyridine (**1**)⁺, 2,6-bis(*N,N*-dimethylaminomethyl)pyridine (**2**)⁺, 2,6-di-2'-pyridylphenyl (**3**)⁰, or 2-(2,2'-bipyridin-6-yl)phenolato (**4**)⁰), and dicarbonylruthenium complexes with two semiquinone ligands, $[\text{Ru}(\text{CO})_2(\text{sq})_2]$ (**5**)⁰ and $[\text{Ru}(\text{CO})_2(\text{phsq})_2]$ (phsq = 9,10-phenanthrasemiquinone, **6**)⁰, were synthesized and the structures of **1**⁺ and **6** were determined by x-ray crystal anal. Monocarbonyl Ru(II)-dioxolene complexes displayed the ligand localized catecholato/semiquinone and semiquinone/quinone redox couples, and two sets of those redox couples were obsd. in the dicarbonyl Ru(II)-bis(dioxolene) complexes. Spectroelectrochemical study revealed that the Ru(II)-catecholato and Ru(II)-semiquinone complexes were stable in

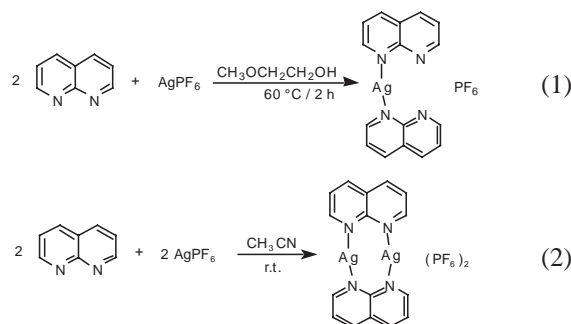
solutions, while the Ru(II)-quinone complexes underwent fragmentation in solutions. One-electron reduction of the monocarbonyl Ru(II)-semiquinone complexes caused a red shift of the $\nu(\text{CO})$ bands at 41–56 cm^{-1} , which was substantially larger than those of carbonyl Ru(II)-polypyridyl complexes. Two $\nu(\text{CO})$ bands of dicarbonyl Ru(II)-bis(semiquinone) complexes also shifted to lower wavenumber at 53–99 cm^{-1} upon two electron reduction of the complexes. The unusually large red shift of $\nu(\text{CO})$ bands upon redn. of carbonyl Ru(II)-dioxolene complexes compared with those of Ru(II)-polypyridyl complex is ascribed to a strong electronic interaction between carbonyl and dioxolene ligands.

VIII-F-10 Synthesis and Crystal Structures of Mono- and Dinuclear Silver(I) Complexes Bearing 1,8-Naphthyridine Ligand

KOIZUMI, Take-aki; TANAKA, Koji

[*Inorg. Chim. Acta* **357**, 3666–3672 (2004)]

Mononuclear and dinuclear silver(I) complexes bearing 1,8-naphthyridine (napy) were prepared. The crystal structures of $[\text{Ag}(\text{napy-}\kappa\text{N})_2](\text{PF}_6)$ (**1**) and $[\text{Ag}_2(\mu\text{-napy})_2](\text{PF}_6)_2 \cdot 3\text{CH}_3\text{CN}$ (**2**·3CH₃CN) were determined by X-ray diffraction studies. In complex **1**, intermol. π - π interaction of napy ligands between neighboring molecules forms left-handed hexagonal columns in the solid state. On the other hand, two napy ligands bridging two Ag ions in the dinuclear complex **2** shape a face-to-face π - π stacking with those of the neighboring molecule to form the dimeric unit. Besides, two of four napy ligands, which are located in a diagonal position in the dimeric unit, build intermolecular back-to-back π - π stackings with those of the adjacent dimeric unit, and a ladder-like stairway structure is generated in the solid state. Irrespective of such characteristic structures of **1** and **2** in the solid state, both complexes show very rapid dynamic behavior in solutions. No conversion between **1** and **2** took place even in the presence of excess amounts of Ag⁺ or napy in solutions.



VIII-G Silanechalcogenolato Complexes

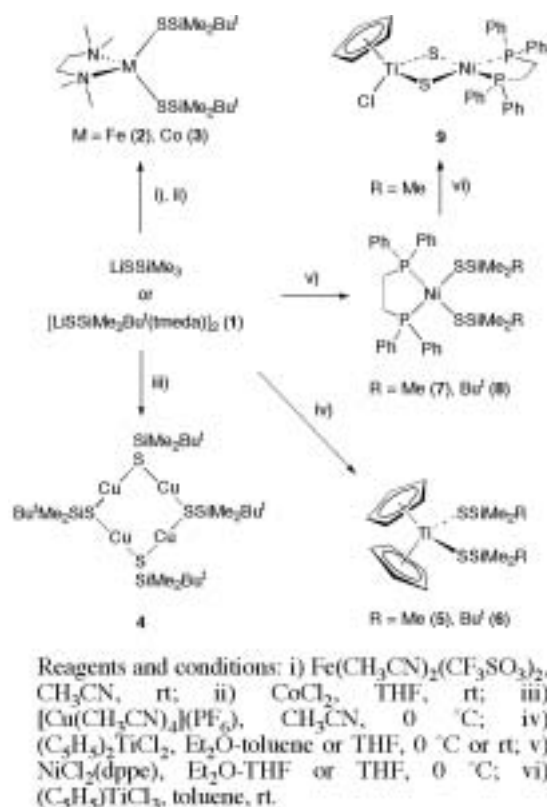
The development of synthetic routes to mixed-metal chalcogenido clusters is a critical prerequisite for study of these important materials. It is well known that $(\text{Me}_3\text{Si})_2\text{E}$ ($\text{E} = \text{S}, \text{Se}, \text{Te}$) is a good chalcogen transfer reagent, which can replace a halide, alkoxide, acetate, and oxide with a chalcogen ligand by taking advantage of formation of Si–Cl and Si–O bonds. Therefore the corresponding M–ESiMe₃ species hold great promise for synthetic precursors of chalcogenido clusters. One of the important advantages of using this system is the possibility of controlling cluster-forming reactions by the choice of steric and electronic properties of the substituents on silicon. This approach has been widely used in organic syntheses, where silyl groups have proven to be useful as protecting agents of functional groups under various conditions. However, because of the high lability of Si–E bond, there is a strong tendency to restrict the use of silanechalcogenolato complexes. In this project, we have studied chemistry of silanechalcogenolato complexes, aiming at developing the rational synthesis of chalcogenido clusters.

VIII-G-1 Synthesis and Structural Characterization of Silanethiolato Complexes Having *tert*-Butyldimethylsilyl and Trimethylsilyl Groups

KOMURO, Takashi¹; MATSUO, Tsukasa;
KAWAGUCHI, Hiroyuki; TATSUMI, Kazuyuki¹
(¹Nagoya Univ.)

[Dalton Trans. 1618–1625 (2004)]

Treatment of cyclotrisilathiane $(\text{Me}_2\text{SiS})_3$ with 3 equiv of RLi ($\text{R} = \text{Me}, \text{Bu}^t$) in hexane–Et₂O afforded the lithium silanethiolates LiSSiMe₂R, and the tmeda adduct $[(\text{tmeda})\text{LiSSiMe}_2\text{Bu}^t]_2$ **1** (tmeda = *N,N,N',N'*-tetramethylethylenediamine) was isolated in the case of $\text{R} = \text{Bu}^t$. Reaction of $\text{Fe}(\text{CH}_3\text{CN})_2(\text{CF}_3\text{SO}_3)_2$, CoCl_2 , and $[\text{Cu}(\text{CH}_3\text{CN})_4](\text{PF}_6)$ with **1** gave rise to the silanethiolato complexes $\text{M}(\text{SSiMe}_2\text{Bu}^t)_2(\text{tmeda})$ ($\text{M} = \text{Fe}$ **2**, Co **3**), and $[\text{Cu}(\text{SSiMe}_2\text{Bu}^t)]_4$ **4**, respectively. Complexes $(\text{C}_5\text{H}_5)_2\text{Ti}(\text{SSiMe}_2\text{R})_2$ ($\text{R} = \text{Me}$ **5**, Bu^t **6**) and $\text{Ni}(\text{SSiMe}_2\text{R})_2(\text{dppe})$ [$\text{R} = \text{Me}$ **7**, Bu^t **8**; dppe = 1,2-bis(diphenylphosphino)ethane] were prepared from treatments of $(\text{C}_5\text{H}_5)_2\text{TiCl}_2$ and $\text{NiCl}_2(\text{dppe})$ with the corresponding lithium silanethiolates. Complex **7** readily reacted with $(\text{C}_5\text{H}_5)_2\text{TiCl}_3$ to produce the Ti–Ni heterobimetallic compound $(\text{C}_5\text{H}_5)_2\text{TiCl}(\mu\text{-S})_2\text{Ni}(\text{dppe})$ **9**, in which silicon–sulfur bond cleavage took place.



VIII-H Coordination Chemistry of Sterically Hindered Ligands and Multidentate Ligands, and Activation of Small Molecules

This project is focused on the design and synthesis of new ligands that are capable of supporting novel structural features and reactivity. Currently, we are investigating multidentate ligands based on aryloxy, thiolate, and amidinate. In addition, we set out to study metal complexes with sterically hindered arylthiolate ligands. Our recent efforts have been directed toward activation of small molecules.

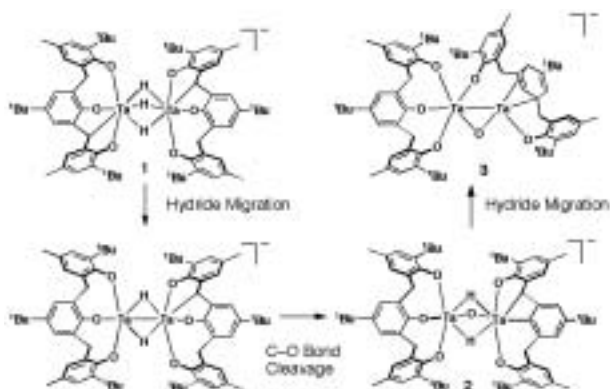
VIII-H-1 Aryl-Oxygen Bond Cleavage by a Trihydride-Bridging Ditantalum Complex

KAWAGUCHI, Hiroyuki; MATSUO, Tsukasa

[J. Am. Chem. Soc. **125**, 14254–14255 (2003)]

Treatment of $[\text{Ta}^t\text{Bu-L}]_2$ with LiBHET_3 gave $[\text{Ta}^t\text{Bu-L}]_2(\text{H})_3\text{Li}(\text{thf})_2$ (**1**). Complex **1** is a Ta(V) dimer, in which two metal center are bridged by three hydride ligands. The formation of **1** is believed to proceed *via* a Ta(III)–Ta(III) intermediate which undergoes intramolecular addition of a methylene CH bond of the

ligand. Complex **1** is thermally unstable and gradually undergoes rearrangement. The first step is likely the migration of one hydride to the methine carbon of the *bit*-^tBu-L ligand to form a dihydride Ta(IV)–Ta(IV) intermediate. Subsequent C–O scission occurs across the metal–metal bond, in which two electrons stored in metal–metal bonding is used to yield an oxo-dihydride dimer **2**. The final formation of **3** requires the migration of two hydrides to a methine and an aryl carbon, respectively. The overall transformation implies an internal redox process and does not require electrons to be added to or removed from **1**.

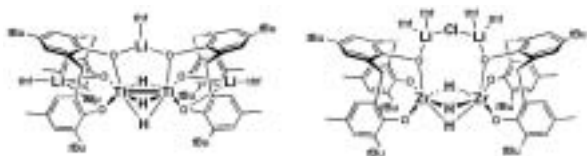


VIII-H-2 Triple Hydrogen Bridged Ditungsten(III) and Dizirconium(IV) Aryloxy Complexes

MATSUO, Tsukasa; KAWAGUCHI, Hiroyuki

[*Organometallics* **22**, 5379–5381 (2003)]

The first example of triple hydrogen bridged ditungsten(III) system, $[\text{Li}_3(\text{thf})_3][\text{Ti}(\text{tBu-L})_2(\mu\text{-H})_3]$ (**2**) supported by the tridentate aryloxy ligand was synthesized by the reaction of $[\text{Ti}(\text{tBu-L})\text{Cl}]_2$ (**1**) with LiBHET_3 [$\text{H}_3(\text{tBu-L}) = 2,6\text{-bis}(4,6\text{-methyl-}t\text{-butyl-salicyl})\text{-4-}t\text{-butylphenol}$]. On the other hand, the analogous reaction of $\text{Zr}(\text{tBu-L})\text{Cl}(\text{thf})_2$ (**3**) yielded the triple hydrogen bridged dizirconium(IV), $[\text{Li}_2\text{Cl}(\text{thf})_4][\text{Zr}(\text{tBu-L})_2(\mu\text{-H})_3]$ (**4**). Structures of **2** and **4** were determined by X-ray crystallography. The titanium dimer adopts a face-sharing bioctahedral geometry with a very short Ti–Ti distance (2.621(1) Å). The diamagnetic nature and the dynamic behavior of **2** in solution were revealed by NMR studies.

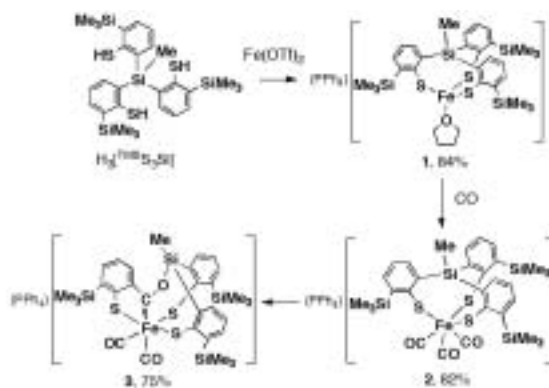


VIII-H-3 Formation of an Iron(II) Carbene Thiolato Complex via Insertion of Carbon Monoxide into Si–C Bond

YUKI, Masahiro; MATSUO, Tsukasa;
KAWAGUCHI, Hiroyuki

[*Angew. Chem., Int. Ed.* **43**, 1404–1407 (2004)]

The reaction of $\text{Fe}(\text{CF}_3\text{SO}_3)_2(\text{CH}_3\text{CN})_2$ with $\text{Li}_3[\text{TMS}_3\text{Si}]$ ($\text{H}_3[\text{TMS}_3\text{Si}] = \text{tris}(3\text{-trimethylsilyl-2-mercaptophenyl)methylsilane}$) followed by addition of PPh_4Br afforded $(\text{PPh}_4)[\text{Fe}(\text{TMS}_3\text{Si})(\text{thf})]$ (**1**). Complex **1** reacted with CO to produce $(\text{PPh}_4)[\text{Fe}(\text{TMS}_3\text{Si})(\text{CO})_3]$ (**2**). The carbonyl compound **2** is thermally unstable in solution. Stirring the solution of **2** at room temperature resulted in formation of the carbene-thiolato complex **3**, in which the insertion of CO into Si–C bond took place. A kinetic study of this reaction showed that this was first order in **2** with the appreciable positive entropy of activation. The crystal structures of **1** and **3** were determined by the X-ray analysis. The most remarkable feature in **3** is that the crystal structure exhibits substantial bonding interaction between the carbene carbon and the thiolato sulfur.



VIII-I Preparation and Properties of the Homo- and Heterometallic Clusters

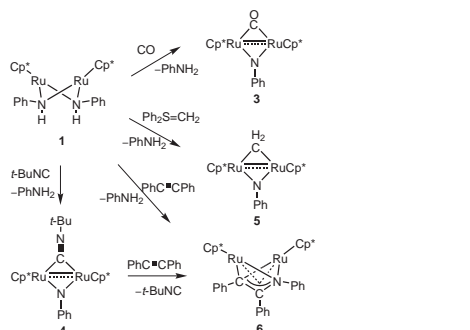
This project focuses on the development of a systematic synthetic route to a series of the homo- and heterometallic clusters as templates or catalysts for new types of activation and transformation of organic, inorganic, and organometallic molecules at the well-defined multimetallic reaction sites. Especially, preparation and reactivity of dinuclear Ru(II) complexes having the bridging amido ligands has been extensively studied.

VIII-I-1 Reactivity of Amido Ligands on a Dinuclear Ru(II) Center: Formation of Imido Complexes and C-N Coupling Reaction with Alkyne

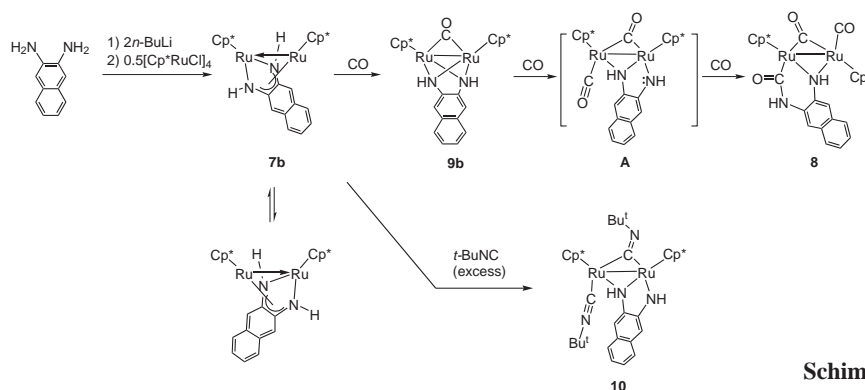
TAKEMOTO, Shin¹; KOBAYASHI, Tomoharu¹; MATSUZAKA, Hiroyuki²
(¹Osaka Prefecture Univ.; ²IMS and Osaka Prefecture Univ.)

[*J. Am. Chem. Soc.* **126**, 10802–10803 (2004)]

Reactions of the dimeric Ru(II) anilido complex [Cp*₂Ru(μ₂-NHPh)]₂ (**1**; Cp* = η⁵-C₅Me₅) with CO, *t*-butyl isocyanide, a sulfur ylide Ph₂S=CH₂, and diphenylacetylene proceeded with an unexpected disproportionation of the μ₂-anilido ligands to form free aniline and a series of new imidodiruthenium complexes **3–5** (Scheme 1). In the case of diphenylacetylene, the imido fragment underwent subsequent coupling reaction with the alkyne to produce an iminoalkenyl complex **6**.



Existence of a Ru–Ru multiple bond is suggested by



Scheme 1.

electron counting and the short Ru–Ru distance that is close to those of some other compounds with Ru=Ru double bonds (2.417–2.629 Å). Orbital analysis of a DFT-B3PW91 optimized model compound [(CpRu)₂(μ₂-CO)(μ₂-NH)] (**3'**) has provided insights into the Ru–Ru bond in **3**. Although the first six of HOMOs of **3'** are predominantly metal-based orbitals and constitute a formally nonbonded σ²σ*²δ⁴σ*⁴ configuration, the multiple bond order between the Ru atoms can be rationalized by back-donation from the filled Ru–Ru σ* orbital into a π* orbital of the CO ligand, and by donation from the imido and CO ligands into empty Ru–Ru π-bonding orbitals.

VIII-I-2 A Dinuclear Ru(II) Chelating Amido Complex: Synthesis, Characterization, and Coupling Reaction with Carbon Monoxide

TAKEMOTO, Shin¹; OSHIO, Shinya¹; KOBAYASHI, Tomoharu¹; MATSUZAKA, Hiroyuki²; HOSHI, Masatsugu³; YAMASHITA, Masayo³; MIYASAKA, Hitoshi³; ISHII, Tomohiko³; YAMASHITA, Masahiro³
(¹Osaka Prefecture Univ.; ²IMS and Osaka Prefecture Univ.; ³Tokyo Metropolitan Univ.)

[*Organometallics* **23**, 3587–3589 (2004)]

Results are summarized in Scheme 1. [Cp*₂RuCl]₄ (Cp* = η⁵-C₅Me₅) reacts with 2 equiv of dilithium 2,3-naphthalenediamide to afford a dinuclear bridging amido complex **7b** in moderate yield. Treatment of **7b** with CO (1 atm) resulted in the incorporation of three molecules of CO into the diruthenium core to give a carbamoyl amido bis(carbonyl) complex **8**. Similar treatment of **7b** with *tert*-butyl isocyanide resulted in the quantitative formation of a bis(isocyanide) complex **10**, in which the two amido nitrogen atoms also occupy the terminal and bridging coordination sites.

VIII-J Synthesis of Transition Metal Complexes Containing a Novel Metal-Silicon and Metal-Gallium Bonding

Synthesis of transition metal complexes with unprecedented bonds between a metal and a heavy main group element is one of current topics on inorganic chemistry. In this project, we have investigated the synthesis, structure, and reactivities of metal complexes containing metal-silicon and metal-gallium unsaturated bonding. We also investigated germylene-bridged diiron complexes having a triplet ground state.

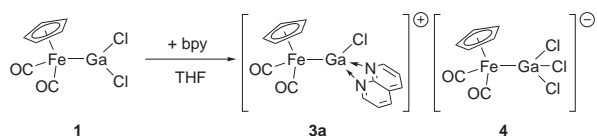
VIII-J-1 Synthesis, Structure, and Reactivity of Cationic Base-Stabilized Gallyleneiron Complexes

UENO, Keiji¹; WATANABE, Takahito²; OGINO, Hiroshi³

(¹IMS and Gunma Univ.; ²Tohoku Univ.; ³Univ. Air)

[*Appl. Organomet. Chem.* **17**, 403–408 (2003)]

Addition of 2,2'-bipyridine (bpy) to an acetonitrile solution of dichlorogallyliron complex FpGaCl_2 (**1**: $\text{Fp} = (\eta\text{-C}_5\text{H}_5)\text{Fe}(\text{CO})_2$) afforded almost quantitatively a salt consisting of a cationic base-stabilized gallylene complex $[\text{FpGaCl}\text{-bpy}]^+$ (**3a**) and an anionic complex $[\text{FpGaCl}_3]^-$ (**4**). Reaction of $\text{Fp}'\text{GaCl}_2$ ($\text{Fp}' = \text{Fp}$ (**1**), Fp^* (**2**); $\text{Fp}^* = (\eta\text{-C}_5\text{Me}_5)\text{Fe}(\text{CO})_2$) with NaBPh_4 in the presence of a bidentate donor (Do_2) gave $[\text{Fp}'\text{GaCl}\text{-Do}_2]\text{BPh}_4$ where Do_2 was bpy or 1,10-phenanthroline (phen). These cationic complexes may be useful precursors for the synthesis of gallyleneiron complexes with various substituents on the gallium atom. Indeed, reaction of $[\text{Fp}^*\text{GaCl}\text{-phen}]\text{BPh}_4$ (**5b**) with NaS^PTol or $\text{Me}_3\text{SiS}^P\text{Tol}$ afforded the gallyleneiron complex $[\text{Fp}^*\text{GaS}^P\text{Tol}\text{-phen}]\text{BPh}_4$ (**6**), the first example of a gallium-transition metal complex having a thiolate group on the gallium atom. The molecular structures of **5b** and **6** were determined by single crystal X-ray diffraction.



VIII-J-2 Synthesis and Structure of the First Dinuclear Complex Bridged by a Substituent-Free Gallium Atom

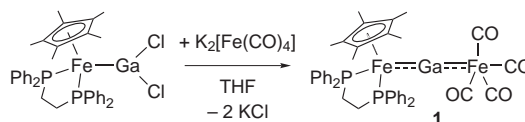
UENO, Keiji¹; WATANABE, Takahito²; TOBITA, Hiromi²; OGINO, Hiroshi³

(¹IMS and Gunma Univ.; ²Tohoku Univ.; ³Univ. Air)

[*Organometallics* **22**, 4375–4377 (2003)]

The first dinuclear complex bridged by a substituent-free gallium atom, $\text{Cp}^*\text{Fe}(\text{dppe})(\mu\text{-Ga})\text{Fe}(\text{CO})_4$ (**1**, $\text{Cp}^* = \eta\text{-C}_5\text{Me}_5$, $\text{dppe} = \text{Ph}_2\text{PCH}_2\text{CH}_2\text{PPh}_2$), was synthesized by the reaction of $\text{Cp}^*\text{Fe}(\text{dppe})\text{GaCl}_2$ with $\text{K}_2[\text{Fe}(\text{CO})_4]$. Crystal structure analysis of complex **1** revealed that the geometry around the gallium atom is essentially linear and the Fe–Ga bonds are significantly shorter than that of usual single bonds. These structural features

indicate that the Fe–Ga bonds bear significantly unsaturated character.



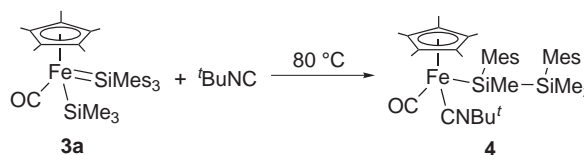
VIII-J-3 Direct Evidence for Extremely Facile 1,2- and 1,3-Group-Migrations on an FeSi_2 System

TOBITA, Hiromi¹; MATSUDA, Akihisa¹; HASHIMOTO, Hisako¹; UENO, Keiji²; OGINO, Hiroshi³

(¹Tohoku Univ.; ²IMS and Gunma Univ.; ³Univ. Air)

[*Angew. Chem., Int. Ed.* **43**, 221–224 (2004)]

Photolysis of $[\text{Cp}'\text{Fe}(\text{CO})_2\text{Me}]$ (**1a**: $\text{Cp}' = \eta^5\text{-C}_5\text{Me}_5$ (Cp^*); **1b**: $\text{Cp}' = \eta^5\text{-C}_5\text{H}_5$ (Cp)) in the presence of $\text{HSiMe}_2\text{SiMe}_2\text{SiMe}_2\text{Me}$ (**2**; $\text{Mes} = \text{mesityl}$ (2,4,6-trimethylphenyl)) produced the first donor-free silyl(silylene)iron complexes $[\text{Cp}'\text{Fe}(\text{CO})(=\text{SiMe}_2)\text{SiMe}_3]$ (**3a**: $\text{Cp}' = \text{Cp}^*$, 60%; **3b**: $\text{Cp}' = \text{Cp}$, 38% yield, calculated by NMR spectroscopy). Complex **3a** was isolated as orange crystals in 40% yield, whereas isolation of **3b** was unsuccessful. When **3a** was heated to 80 °C for 6 h in the presence of $t\text{BuNC}$, a disilanyl complex $[\text{Cp}^*\text{Fe}(\text{CO})(\text{CN}^t\text{Bu})\text{SiMe}(\text{SiMe}_2)]$ (**4**) was isolated as a main product in 25% yield. These results provide the most straightforward evidence for extremely facile 1,2- and 1,3-group migrations of the substituents between two silicon atoms in silyl(silylene) complex systems.



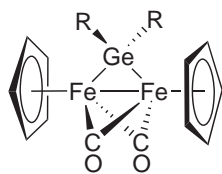
VIII-J-4 Synthesis and Characterization of Triplet Germylene-Bridged Diiron Complexes and Singlet Stannylene-Bridged Diiron Complexes

MOHAMED, Bahaa. A. S.¹; KIKUCHI, Mami¹; HASHIMOTO, Hisako¹; UENO, Keiji²; TOBITA, Hiromi¹; OGINO, Hiroshi³

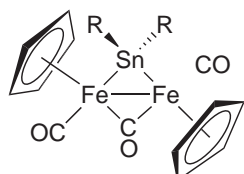
(¹Tohoku Univ.; ²IMS and Gunma Univ.; ³Univ. Air)

[*Chem. Lett.* **33**, 112–113 (2004)]

Photoreaction of $\text{CpFe}(\text{CO})_2\text{Me}$ with sterically congested R_2GeH_2 [$\text{R} = 2,4,6\text{-C}_6\text{H}_2\text{Pr}_3$ (Tip), $2,4,6\text{-C}_6\text{H}_2\text{Me}_3$ (Mes)] afforded paramagnetic gerylene-bridged diiron complexes having a triplet ground state, $\text{Cp}_2\text{Fe}_2(\mu\text{-CO})_2(\mu\text{-GeR}_2)$ (**3a**, $\text{R} = \text{Tip}$; **3b**, $\text{R} = \text{Mes}$), while the analogous reaction with R_2SnH_2 afforded diamagnetic complexes $\text{Cp}_2\text{Fe}_2(\text{CO})_2(\mu\text{-CO})(\mu\text{-SnR}_2)$ (*trans*-**5a**, $\text{R} = \text{Tip}$; *trans*-**5b**, $\text{R} = \text{Mes}$). The structure of **3a** was determined by X-ray crystallography.



3: $\text{R} = \text{Tip}, \text{Mes}$



trans-**5**: $\text{R} = \text{Tip}, \text{Mes}$